C_6H_6/Au(111): Interface dipoles, band alignment, charging energy, and van der Waals interaction

E. Abad,[1,a)] Y. J. Dappe,[2] J. I. Martínez,[1,b)] F. Flores,[1] and J. Ortega[1]
[1]*Departamento de Física Teórica de la Materia Condensada, Universidad Autónoma de Madrid, ES-28049 Madrid, Spain*
[2]*Institut de Physique et Chimie des Matériaux de Strasbourg, UMR 7504 (CNRS-Université de Strasbourg), 67034 Strasbourg, France*

(Received 23 July 2010; accepted 6 November 2010; published online 24 January 2011)

We analyze the benzene/Au(111) interface taking into account charging energy effects to properly describe the electronic structure of the interface and van der Waals interactions to obtain the adsorption energy and geometry. We also analyze the interface dipoles and discuss the barrier formation as a function of the metal work-function. We interpret our DFT calculations within the induced density of interface states (IDIS) model. Our results compare well with experimental and other theoretical results, showing that the dipole formation of these interfaces is due to the charge transfer between the metal and benzene, as described in the IDIS model. © *2011 American Institute of Physics*. [doi:10.1063/1.3521271]

I. INTRODUCTION

The performance of organic multilayer devices, already existing in the market, depends critically on the energy barriers that control the carrier transport between layers; these barriers are determined by the relative alignment of the molecular levels at metal–organic (MO) or organic–organic (OO) interfaces.[1,2] These interface level alignments have been widely investigated in the last decade: since the Schottky–Mott limit (where use of the vacuum level alignment is made) was disproved[3,4] many different mechanisms have been proposed to explain the barrier formation at MO interfaces: chemical reactions and the formation of gap states in the organic gap;[5–8] orientation of molecular dipoles;[9,10] or compression of the metal electron tails at the MO interface due to the Pauli repulsion.[7,11–13] It has also been suggested that the tendency of the charge neutrality level (CNL) of the organic material to align with the interface Fermi level[14,15] plays also an important role; this mechanism is associated with the induced density of interface states (IDIS) and the charge transfer between the organic and the metal. More recently, this model has been extended to the unified-IDIS model by inclusion of the Pauli repulsion and intrinsic molecular dipoles.[13,16]

In this paper we consider the case of a benzene/Au(111) interface and analyze its barrier height for an isolated molecule and a full monolayer (see Fig. 1); Several authors have analyzed theoretically the benzene/Au interface using other techniques:[12,17,18] Bagus and co-workers have used the constrained space orbital variation method, while Morikawa and co-workers have used a density functional theory-general gradient approximation (DFT-GGA) approach. We reconsider this case because of an extra problem appearing when analyzing organic interfaces: the point is that neither standard GGA- or local density approximation (LDA)-DFT calculations yield an appropriate description of the organic transport energy gap.[19,20] In particular, the Kohn–Sham eigenvalues calculated using the LDA or GGA exchange-correlation functionals yield a transport gap that is too small. It has been argued elsewhere[21–23] that the effective charging energy of the molecule, U, can be used to correct the Kohn–Sham energy gap, E^{KS}, to yield the following transport gap:

$$E^t = E^{KS} + U, \tag{1}$$

an equation that will be used below to determine E^t self-consistently.

In our approach we analyze the benzene/Au(111) interface by combining a LDA-DFT method with a calculation of the charging energy, U, of the molecule, to obtain the appropriate transport energy gap using Eq. (1). We also analyze the interface dipoles and discuss the barrier formation as a function of the metal work-function. We interpret our DFT calculations within the unified-IDIS model and show how our results can be understood in terms of the molecule CNL and a screening parameter, S, operating at the interface level.[20] In Sec. II, we present our calculational method and discuss in detail the benzene/Au interaction energy, taking into account van der Waals forces. In Sec. III we present our DFT results for the isolated molecule and a monolayer coverage, including charging energy effects. In Sec. IV, we discuss the pillow and "metal surface" dipole corrections to our results and, finally, in Sec. V we present our conclusions.

II. BENZENE/AU INTERACTION. DFT AND VAN DER WAALS CORRECTION

A. Method of calculation

We analyze the benzene/Au(111) interface by means of a very efficient DFT tight binding molecular dynamics (TBMD) technique (FIREBALL).[24] In these calculations

a)Electronic mail: enrique.abad@uam.es.
b)Electronic mail: joseignacio.martinez@uam.es.

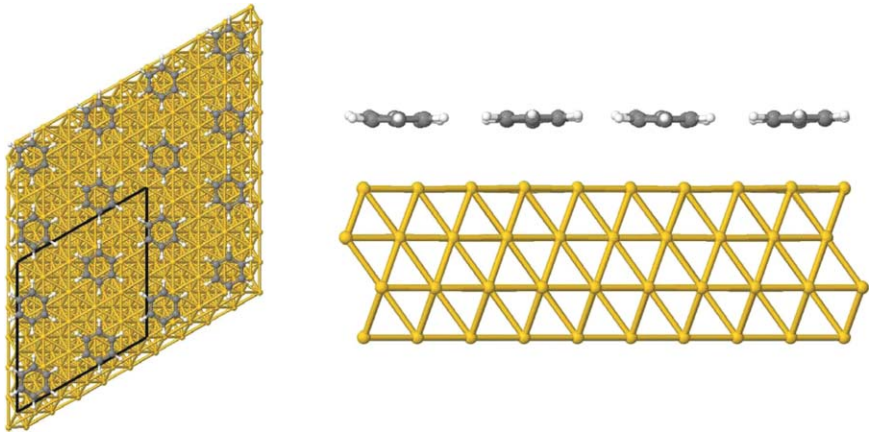

FIG. 1. Left: 5×5 benzene/Au(111) monolayer structure used in the calculations of this paper. Black line indicates the boundaries of the unit cell. Right: 8×8 cluster used to simulate the surface.

the LDA exchange-correlation functional is used as a first-approximation that is corrected in a second step to properly take into account van der Waals forces (see below). A basis set of optimized numerical atomic orbitals[25] (NAOs) is used to represent the valence electrons, while the core electrons are taken into account by means of pseudopotentials.[26] For benzene we have used a minimal sp^3 basis set of optimized NAOs, see Ref. 25. This yields a C-C nearest neighbors distance of 1.40 Å [to be compared with the experimental value of 1.392 Å (Ref. 27)], and a highest occupied molecular orbital/lowest unoccupied molecular orbital (HOMO/LUMO) energy gap of 6.1 eV, to be compared with 4.7 eV for converged basis set LDA or GGA calculations.[18] For Au, we use a basis set of sp^3d^5 NAOs (to represent the 11 valence electrons per atom) with the following cut-off radii [in atomic units (a.u.)]: $s = 4.5$, $p = 4.9$, $d = 4.3$ (Au) [that yields a bulk gold lattice parameter of 4.12 Å versus a experimental value of 4.07 Å (Ref. 28)]. This basis set has been optimized to yield a good description of the electronic band structure as well as atomic structure for bulk Au and has been used in previous studies on the interaction of Au-tips with C_{60} and C_{60}/Au(111) interface.[21,23] The main inaccuracy of this "minimal basis" approach, once the basis has been optimized for each subsystem, appears in the relative initial alignment of the electronic levels for both materials; this problem is corrected in our approach, using a shift operator, as discussed below.

The geometry used in our calculations for the monolayer case (see Fig. 1) is inspired on the $\sqrt{52} \times \sqrt{52}$ experimental structure for this interface.[29] In order to simulate it we have followed a supercell approach with 5×5 periodicity in the xy plane, and four C_6H_6 molecules in the unit cell. This structure has the same hexagonal neighbor structure than the $\sqrt{52} \times \sqrt{52}$ experimental structure and similar benzene–benzene distance (7.3 Å versus experimental value of 6.95 Å), so that the main difference is that our coverage is slightly smaller (∼10%) than the experimental monolayer. Calculations were performed for slabs of six and four Au layers; in particular we found that four Au-layers are enough to obtain converged results for the electronic structure of the interface.[30] We have used eight special k-points for the Brillouin zone sampling. The C_6H_6/Au(111) geometry was first relaxed at the LDA level keeping the three lower Au layers fixed, while the first three layers were allowed to relax.

For the case of the isolated C_6H_6 molecule on Au(111), the Au(111) surface is simulated by means of a cluster of 256 Au-atoms, with four Au-layers and 64 atoms per layer, with 8×8 arrangement (see Fig. 1; it has been checked that this cluster size is enough to avoid border effects. Since only minor internal atomic displacements (less than 0.05 Å) were observed in the relaxation for the periodic case, we kept the internal geometry of molecule and surface fixed, and only changed their vertical distance; this approximation is also used when van der Waals forces are included in the calculations, see Fig. 2 .

The main approximations of our DFT approach are:

(a) The use of the LDA exchange-correlation functional; as mentioned above, this yields transport gaps that are usually too small. For example, the Kohn–Sham LDA HOMO/LUMO energy gap for the gas-phase

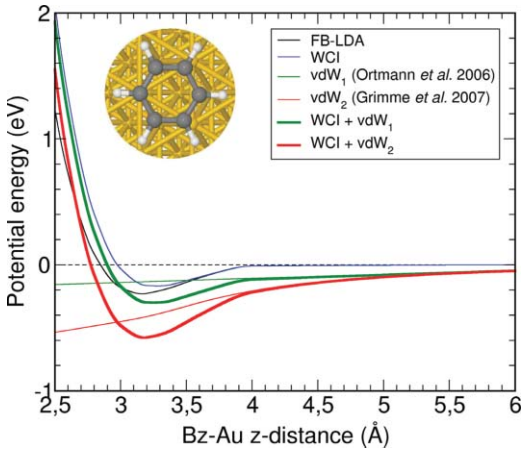

FIG. 2. Energy vs distance for the benzene/Au(111) interaction. Thin black line: standard LDA-FIREBALL (FB-LDA) calculation. Thin blue line: weak chemical interaction (WCI) calculated as discussed in the text. Thin green and red lines: two different parameterizations (Refs. 31 and 32) of the van der Waals (vdW_1 and vdW_2) interaction. Thick green and red lines: total benzene-Au interactions (WCI + vdW_1 and WCI + vdW_2).

benzene molecule is $E^{KS} = 4.7$ eV, while the experimental HOMO/LUMO energy gap (i.e., the difference between the affinity level and ionization potential) is 10.3 eV. On the other hand, as LDA-DFT exchange-correlation functionals do not take into account properly weak London dispersive forces, in physisorbed systems (like the one considered in this work) LDA adsorption energies and distances are not fully reliable.

(b) In the FIREBALL approach a self-consistent version of the so-called Harris–Foulkes functional is used; in this approximation the Kohn–Sham potential is calculated by approximating, in a self-consistent fashion, the total input charge by a superposition of spherical charges around each atom.

(c) The use of a nonfully converged basis set of NAOs.

In the present calculations we correct the deficiencies introduced by these approximations in the following way:

(1) We correct the transport gap using Eq. (1). The point to stress here is that in order to determine U, we have first analyzed the case of an isolated molecule on the surface; from our DFT-LDA calculation, U can be related to the potential induced in the molecule, V^{IDIS} (see below), and to the number of electrons transferred to it, n, by the equation $U = eV^{IDIS}/n$.[21] Then, E^t is calculated by introducing in our Hamiltonian the following scissor operator, $\mathbf{O}^{scissor} = U/2 \sum_{\mu_i,\nu_i} \{|\mu_i\rangle\langle\mu_i| - |\nu_i\rangle\langle\nu_i|\}$, $|\mu_i\rangle$ ($|\nu_i\rangle$) being the empty (occupied) orbitals of the isolated, but deformed, molecule (with the actual geometry of the molecule on the surface).[21] Obviously U depends on E^t, and this forces us to calculate E^t and U self-consistently. Once we have determined U from the single molecule case, we calculate the monolayer case by introducing the same scissor operator which, in this way, takes into account the molecule charging effects. We also use $\mathbf{O}^{scissor}$ to correct the error in the LDA gap due to the basis set.

(2) In order to have the Au and benzene levels correctly aligned initially at the experimental value, we shift by ε_0 the molecular levels of benzene, using this operator $\mathbf{O}^{shift} = \varepsilon_0 \sum_{\mu_i} |\mu_i\rangle\langle\mu_i|$ ($|\mu_i\rangle$ being the eigenstates of the isolated molecule); as the experimental values of the benzene affinity and ionization levels are -1.14 eV and 9.24 eV,[33,34] respectively, we locate the benzene mid-gap at 4.05 eV from the vacuum level, namely, 1.15 eV above the metal work-function. We also use $\mathbf{O}^{shift}$ to change Φ_M fictitiously in the analysis presented in Sec. III.

(3) Approximation (2) above neglects off-diagonal contributions of the induced charge (dipolar contributions) whose effects, although not important for the self-consistent calculation itself, introduces non-negligible contributions to the induced Hartree potential. One of these effects is associated with the induced "pillow" dipole, which is created by the compression of the electron metal tails due to their overlap with the organic molecule wave-functions.[13] The second effect we consider in this paper is associated with the charge induced on the metal surface and the accompanying induced metal surface dipole,[23] that tends to shift that surface charge from practically the last metal layer to the image plane located outwards. These two effects will be introduced perturbatively below, in Sec. IV, after presenting our DFT-LDA results.

(4) In order to obtain a more reliable benzene/Au adsorption distance and energy, we take into account the molecule/surface van der Waals interaction, as discussed in the following subsection.

B. Interaction energy and van der Waals forces

Weakly interacting systems, such as benzene/Au(111), cannot be characterized accurately in a standard DFT formalism. The reason is that the van der Waals interaction is nonlocal and long-range, while exchange-correlation functionals in standard DFT methods are local and short range, with a typical exponential decay. Therefore, a lot of effort has been directed in recent years to develop a practical DFT approach that properly takes into account van der Waals interactions for these systems (see, e.g., Refs. 31, 32, 35–37, and 38).

In order to accurately determine the equilibrium distance and the binding energy of benzene adsorbed on a gold surface, we have used here an extension of the LCAO-S^2 + vdW formalism, previously developed for noble gases and graphitic materials.[39–41] Within this formalism, we consider two opposite contributions, namely a weak chemical interaction and the attractive van der Waals interaction. The first one is due to the small overlaps between the electronic densities of the two subsystems, leading to a small covalence which is repulsive in the case of graphitic materials.[40–42] This contribution has been treated perturbatively, by expanding the wave-functions and consequently the operators with respect to the overlaps. The second contribution arises from the charge fluctuations in each subsystem, which generate quantum dipole–dipole interactions. This interaction between dipoles is also treated perturbatively.

In the present case, we go beyond the S^2 overlap expansion, and calculate the weak chemical interaction, (i.e., the interaction energy without van der Waals forces) correcting the LDA exchange-correlation energy by defining an electron density for each subsystem and approximating the LDA exchange-correlation energy as the sum of the exchange-correlation energies for the different subsystems, i.e., we neglect in the calculation of the LDA exchange-correlation intramolecular terms the overlap of the densities coming from other subsystems (details will be published elsewhere); this 'corrected' LDA interaction energy is used as an approximation to the weak chemical interaction. Thus, by adding the WCI to the vdW interaction we avoid a possible overcounting of the correlation energy that might appear if we calculate the interaction energy as a sum of LDA+vdW contributions. This approach of adding dispersion forces to a corrected DFT functional is similar to the one proposed in Ref. 35. Regarding the van der Waals part, we have used a generalization of our previous works by considering a typical atom–atom interaction with the standard form $-f_D(R)C_6/R^6$ (R is the distance between atoms). The C_6 coefficients for the C-Au and

H-Au pair of atoms have been calculated using London theory as a guide to extrapolate the coefficient as calculated for the C-C interaction on graphitic materials.[31] This approximation for the C_6 coefficient has already been used successfully in other systems[43] where a value $C_6 = 36$ eV Å^6 is obtained. The factor $f_D(R)$ eliminates the van der Waals contribution for short distances.[31,32] We are going to use two different damping factors common in literature. The first one has the form $f_D(R) = 1 - \exp(-\alpha(R/R_0)^8)$. Following Refs. 31 and 43, we take $\alpha = 7.5 \times 10^{-4}$, and $R_0 = 2.3$ Å. The second one has the form $f_D(R) = 1/(1 + \exp(-d(R/R_0) - 1))$ (Ref. 32) where $d = 20$ and R_0 is the sum of van der Waals radii of the elements under consideration, that is around 3.3 Å.[32]

The results of these calculations for a benzene monolayer on Au(111) are presented in Fig. 2. We have represented the benzene/Au(111) interaction energy versus the benzene-surface distance in two different ways. First, we did a standard FIREBALL LDA calculation (black curve, FB-LDA), which gives a binding energy of around 0.20 eV, clearly insufficient to describe the benzene adsorption on gold. As expected, since the van der Waals contribution is not included in this calculation, we cannot recover the experimental results. In a second step, we have determined the binding energy, considering our generalized LCAO-S^2+ vdW model. The thin blue curve corresponds to the WCI energy as approximated by the corrected LDA interaction energy, the green and red curves to the vdW interaction with Ortmann *et al.*[31] and Grimme[32] parameterizations for the damping factor $f_D(R)$, and the thick green and red lines the sum of both contributions, i.e., the binding energy of the system for both parameterizations. In this way, we obtain an equilibrium distance of around 3.25 Å. The binding energy per molecule for this distance, which depends on the damping factor $f_D(R)$ used, is 0.30 eV using the parameterization by Ortmann *et al.*[31] and 0.60 eV for the parameterization by Grimme.[32] The second energy is in good agreement with the experimental evidence,[44] and the Au/benzene distance is similar to the one found in other calculations.[18] We should point out that, although different parametrations gives different energy adsorptions, the critical factor for the study of the interface dipole is the benzene/Au distance, which is independent of the choice of $f_D(R)$. Now, considering this equilibrium geometry, we analyze in Sec III. the interface dipole potentials as well as the charge transfer at this interface.

III. DENSITY OF STATES, INTERFACE DIPOLE, AND CHARGING ENERGY

A. Benzene molecule on Au(111)

Figure 3 shows the density of states (DOS) projected onto the molecule orbitals as calculated with our DFT-LDA approach for the case of a single molecule on Au(111). The levels of the isolated molecule are also shown for comparison: notice the level broadening associated with the benzene/metal interaction. The initial metal work-function, Φ_M, has been shifted to E_F, the final Fermi level, due to an induced interface potential of $V^{\text{IDIS}} = 0.32$ eV, associated with a charge transfer of ~ 0.07 electrons from the molecule to the surface and its corresponding dipole of 1.19 D. This induced interface potential is the potential on the molecule due to the charge transfer. Notice that, within the IDIS model, the induced interface potential, V^{IDIS}, tends to shift the Fermi level towards the charge neutrality level (defined as the level satisfying charge neutrality conditions in the molecule DOS),[14] in such a way that:

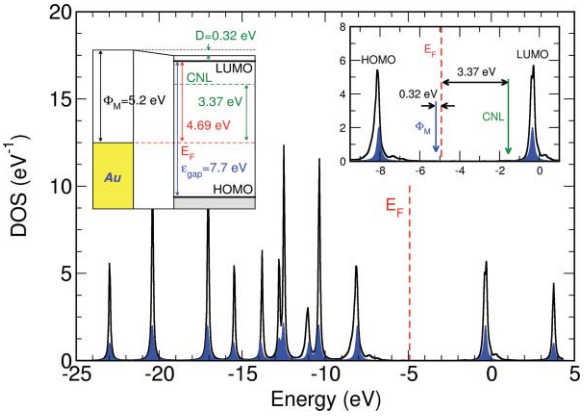

FIG. 3. DOS for a single benzene molecule on Au(111); the initial molecular levels are shown by the blue lines (with a broadening of $\eta = 0.1$ eV). The right inset shows an energy window around the HOMO and LUMO levels indicating the initial work-function, Φ_M, and the CNL. The left inset shows an energy diagram of the benzene/Au interface.

$$\begin{aligned} (\text{CNL} - E_F) &= S(\text{CNL} - \Phi_M), \\ V^{\text{IDIS}} &= (E_F - \Phi_M) = (1 - S)(\text{CNL} - \Phi_M), \end{aligned} \tag{2}$$

S being an interface screening parameter, that for this case is $S = 0.91$. This indicates that the interface screening effect is rather small, a result that is due to: (a) having a very large molecule transport energy gap (7.7 eV), as calculated in the way explained below; and (b) a rather large molecule/metal distance of 3.25 Å.

The transport energy gap of 7.7 eV has been calculated self-consistently using Eq. (1) in the following way: (a) first we calculate for the molecule, using our FIREBALL code, the transport energy gap in LDA ($E^{\text{KS}} = 6.1$ eV; and the HOMO and LUMO levels using the following equations, $E^{\text{LUMO}} = E(N+1) - E(N)$ and $E^{\text{HOMO}} = E(N) - E(N-1)$, $E(N_i)$ being the ground state of the molecule with N_i electrons. These two levels yield $E^t = E^{\text{LUMO}} - E^{\text{HOMO}}$ and the following charging energy, $U = (E^{\text{LUMO}} - E^{\text{HOMO}}) - E^{\text{KS}} = 7.1$ eV for the isolated molecule; (b) in a second step, we calculate within our FIREBALL code, the charging energy for benzene on Au(111); this is given by $(eV^{\text{IDIS}}/n) = 4.8$ eV, so that the molecule charging energy is reduced from 7.1 eV to 4.8 eV, the difference of 2.3 eV being due to surface polarization effects; and (c) finally, the transport energy gap for benzene on Au(111) is obtained by reducing 2.3 eV the HOMO-LUMO gap of the isolated molecule as obtained from the experimental evidence. This yields a transport energy gap of 8.0 eV; this value is still reduced to 7.7 eV due to the metal surface dipole as explained below.

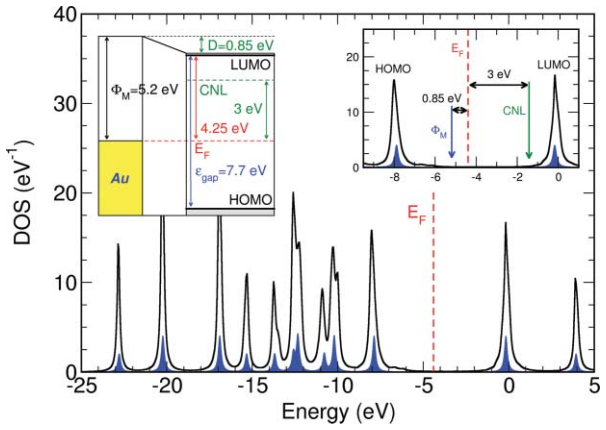

FIG. 4. DOS for a benzene monolayer on Au(111); the initial molecular levels are shown by the blue lines (with a broadening of $\eta = 0.1$ eV). The right inset shows an energy window around the HOMO and LUMO levels, indicating the initial work-function, Φ_m, and the CNL. The left inset shows an energy diagram of the benzene/Au interface.

B. Benzene monolayer on Au(111)

Figure 4 shows our calculated DOS for the geometry of Fig. 1; these results are similar to the ones presented for the isolated molecule, except for the Fermi level position that in this case is located 0.85 eV above the initial metal work-function, with a final Fermi level of 4.40 eV:[23] for this particular case we find, $S = 0.79$, a little smaller than the value given above for the isolated molecule on Au(111). Figure 5 shows also that for a monolayer the interface Fermi level, the interface dipole potential V^{IDIS} and the charge transfer, change linearly with the fictitious metal work-function. The charge transfer from the benzene monolayer to the metal surface is now ~ 0.06 electrons per molecule (a dipole $\mathcal{D}$ of 0.99 D per molecule). This charge transfer is smaller than in the case of

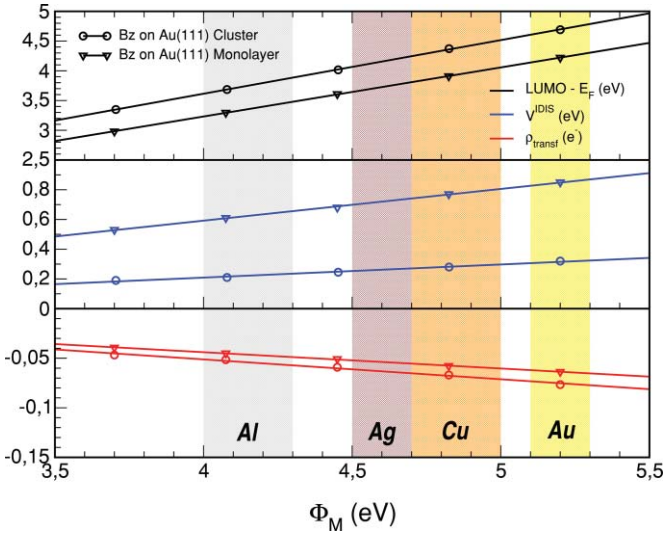

FIG. 5. (LUMO $- E_F$) (upper panel), V^{IDIS} (center panel) and transfer of charge (lower panel) as a function of the "fictitious" metal work-function. The fictitious change in the metal work-function tries to simulate how the interface properties depend on the different metals: this issue is shown in the figure by superimposing the clean metal work-functions of Al, Ag, Cu, and Au for comparison.

a single benzene molecule on Au(111), reflecting the depolarizing effect due to the other benzene molecules. This charge transfer can be used to obtain an average interface dipole potential of $eV^{\mathrm{av}} = 0.81$ eV, using the relation $V^{\mathrm{av}} = 4\pi\mathcal{D}/A$, where A is the surface area per molecule. Notice that eV^{av} is slightly different from the value $eV^{\mathrm{IDIS}} = 0.85$ eV, that corresponds to the potential on each benzene molecule. The relation $V^{\mathrm{av}} = 4\pi\mathcal{D}/A$ has been used to extrapolate the results of cluster calculations to, e.g., the monolayer case, assuming that the dipole per molecule $\mathcal{D}$ is the same in both cases (i.e., neglecting the depolarizing effect for the monolayer). Using the values for $\mathcal{D}$ obtained in our cluster calculation we would obtain $eV^{\mathrm{av}} = 0.97$ eV for our 5×5 monolayer, and $eV^{\mathrm{av}} = 1.05$ eV for the $\sqrt{52} \times \sqrt{52}$ experimental monolayer, values that are very different from the induced interface potential $eV^{\mathrm{IDIS}} = 0.32$ eV obtained for the cluster calculation. Finally, assuming that the dipole per molecule is the same in the 5×5 and $\sqrt{52} \times \sqrt{52}$ structures, yields a dipole potential $eV^{\mathrm{av}} = 0.88$ eV for the $\sqrt{52} \times \sqrt{52}$ case.

IV. PILLOW AND "SURFACE METAL" DIPOLE CORRECTIONS

In this section we consider two effects, not included in our LDA calculation, that are associated with off-diagonal terms of the electron density of states. One is related to the pillow effect, the second one is associated with the charge induced on the metal surface and the accompanying induced metal surface dipole. Both effects are, however, small and it is reasonable to introduce them as a perturbation to our zeroth-order LDA-calculation.

A. Pillow effect

The pillow potential, V^P, is associated with the Pauli exclusion principle between electrons in the organic molecule and the surface. When a molecule is placed over a metal surface, an overlap between both wave functions appear, so that the orthogonalization of those wave functions push the metal electronic tail back into the metal. This charge rearrangement, caused only by orthogonalization leads to a non-negligible dipole that has been previously studied by Bagus and co-workers[45] and Vázquez and co-workers.[13] This dipole, just like the IDIS one, induces a potential drop at the interface characterized by V^P.

In general, this pillow potential, V^P, and the IDIS-potential, V^{IDIS}, define in our case the total interface potential, $V^t = V^P + V^{\mathrm{IDIS}}$, creating the Fermi level shift at the interface: $V^t = E_F - \Phi_M$. We follow Ref. 13 and calculate the pillow dipole by expanding the organic/metal many body interactions up to second order in the wavefunction overlap (that is small for this metal-molecule distance). This leads to the following formula for the dipole $\mathbf{D}_p$ per molecule:[13]

$$\mathbf{D}_p = \sum_{j\in\mathrm{mol},\, j'\in\mathrm{metal},\sigma} -(n_{j\sigma} + n_{j'\sigma})S_{jj'} \int \Delta\mathbf{r}\phi_j\phi_{j'} - (n_{j\sigma} - n_{j'\sigma})S_{jj'}^2 \frac{\mathbf{d}}{4}. \quad (3)$$

In this equation, ϕ_j and $\phi_{j'}$ are the wavefunctions of the molecule and the metal local orbitals, respectively, $S_{jj'}$ is its overlap; and n_j and $n_{j'}$ are their occupancies; $\mathbf{d}$ is the vector joining the atomic positions of orbitals j and j' and $\Delta\mathbf{r}$ joins $\mathbf{d}/2$ with the integration variable $\mathbf{r}$. This equation defines the total pillow dipole; however, in our FIREBALL calculations part of this dipole (in particular the second term) is already taken into account through selfconsistency in the diagonal charges $\{n_{i\sigma}\}$. Thus, we only need to consider here the following off-diagonal contribution:

$$\mathbf{D}'_p = \sum_{j\in\text{mol},\, j'\in\text{metal},\sigma} -(n_{j\sigma} + n_{j'\sigma})S_{jj'} \int \Delta\mathbf{r}\phi_j\phi_{j'}. \quad (4)$$

The pillow potential V^P we include in our calculations is associated with the pillow-dipole given by Eq. (4), which creates a mean potential $V^{P,0}$ between the molecule and the metal. Because of the surface screening, S, we find that:

$$eV^P = SeV^{P,0}, \quad (5)$$

this equation defining the screened pillow potential that we use to calculate the pillow effect in the induced total potential, V^t, and in the Fermi level shift, $E_F - \Phi_M$. In our calculations eV^P is about 0.04 eV for the monolayer and 0.03 eV for the isolated molecule.

B. Metal surface dipole

We pass now to make some comments about the metal surface dipole correction and its effect on our calculations for U. In order to estimate this effect, we first calculate the metal surface dipole using the off-diagonal elements of the Green function as afforded by the tight-binding Hamiltonian obtained from our DFT-LDA calculation as

$$en_{ij} = -\frac{e}{\pi}\int_{-\infty}^{E_F} \Im[G_{ij}(\omega)]d\omega. \quad (6)$$

In the next step, we calculate the potential associated with those off-diagonal terms.[23] This is performed in a simplified calculation by considering only the first metal layer dipoles (all the other layer dipoles are strongly screened) and the mean potential that these dipoles induce between the molecule and the metal. This is a small effect that tends to reduce V^{IDIS}; in the isolated molecule $(E_F - \Phi_M)$ is reduced by 0.02 eV, while for the monolayer the reduction is around 0.05 eV. These effects also reduce U because its variation $\delta V^{\text{surf}}/\delta n$ is negative and have to be added to the calculation of U. In this case $\delta V^{\text{surf}}/\delta n = 0.3$ eV, so, as stated before, the gap is reduced from 8.0 to 7.7 eV. Notice that the dipoles created by the pillow and the metal surface effects have opposite signs, in such a way that both effects tend to cancel each other.

V. DISCUSSION AND CONCLUSIONS

We have presented DFT-LDA calculations for benzene on Au(111) in two limits: an isolated molecule and a full monolayer. The case of an isolated molecule has allowed us to calculate the molecule charging energy, U, and the transport energy gap, E^t, which we have found to be around 7.7 eV. Calculating this energy gap is important for analyzing the interface dipole induced between benzene and Au(111) because large gaps inhibit the charge transfer between both media and reduce the induced interface dipole. In particular, this effect partially explains the differences found between the results presented in this paper for the monolayer limit and the ones published in Ref. 17, where we assumed the transport energy gap to be much smaller, around 4.8 eV; moreover, in that paper we assumed the metal/benzene distance to be much smaller, 2.95 Å, an effect that tends to decrease S and enhances the amount of charge transfer between the molecule and the metal.

Using this energy gap, we have calculated the case of a benzene-monolayer and have found that the metal work-function is reduced an amount of 0.85 eV. This value compares well with the experimental value of 1.1 eV, as given by Bagus and co-workers,[12] although part of the discrepancy might come from some overestimation of the energy gap. To check this point, we have also calculated the monolayer case taking for the benzene molecule an energy gap of 7.0 eV, a value which can still be considered compatible with our previous calculation for E^t taking into account the error bar of 10% appearing in the calculations due to numerical uncertainties related to the small induced DOS at the gap. This value is also suggested by extrapolating the data in Ref. 46 and by semiclassical image potential calculations. Figure 6 shows for this case our calculated DOS projected onto the molecule and the interface barrier; the point to realize is that with the new transport energy gap, the average interface potential eV^{av} has slightly increased from 0.88 to 0.95 eV.

It is also important to discuss the issue of the convergence of our calculations with the basis set. We have studied this convergence by analyzing how our results depend on a more extended basis set; in particular, we have used an extended basis with polarization orbitals, $sp^3d^5s^*d^{*5}$ NAOs for Au, sp^3d^5 for C and ss^* for H with the following cut-off radii (in a.u.): $s = 6.0$, $p = 7.0$, $s^* = 6.0$, $d = 5.0$ and $d^* = 5.0$ (Au); $s = 4.0$, $p = 4.5$, $d = 5.4$(C); and $s = 4.5$, $s^* = 4.5$ (H).[17] Obviously, using this basis set the molecular levels are

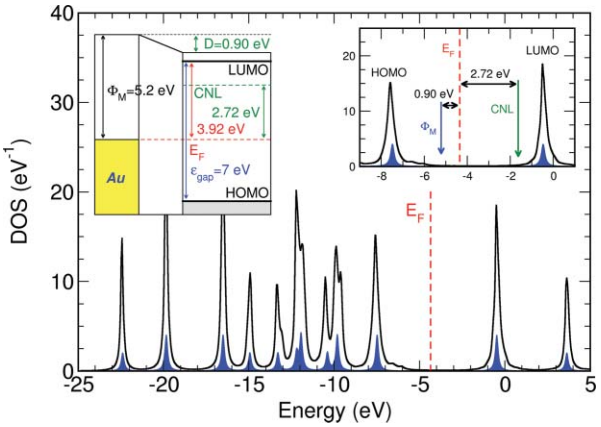

FIG. 6. DOS for a benzene monolayer on Au(111), with a molecule transport energy gap of 7.0 eV; the initial molecular levels are shown by the blue lines. The right inset shows an energy window around the HOMO and LUMO levels, indicating the initial work-function, Φ_M, and the CNL. The left inset shows an energy diagram of the Au/benzene interface.

significantly shifted but, the "scissor" and the "shift" operators discussed above allow us to fit the molecule energy gap and its energy position to the experimental values: we find that using these corrections our calculation of the interface dipole and the charging energy is already reasonably well-converged in our optimized "minimal" basis set calculation, thus allowing us to apply our methodology to the large system sizes typically required for these metal/organic interfaces. An exception to this result is the calculation of the correction discussed in Sec. IV: using this more extended basis increases this correction to 0.40 eV. We conclude that the small difference between our calculated average interface potential, eV^{av} (for a $\sqrt{52} \times \sqrt{52}$ monolayer), 0.88 eV, and the experimental one, 1.1 eV, is probably due to this underestimation of the potential correction.

Finally, we compare our results with other theoretical approaches and with the experimental evidence, looking at the induced interface dipole for benzene (Bz) on Au, Ag and Cu(111). In our calculations, we simulate the Ag and Cu cases by changing the metal workfunction while keeping the Au electronic structure for the metal. From the calculations shown in Fig. 5 (upper panel), we obtain the following interface dipoles: 0.85 eV for Bz/Au(111); 0.69 eV for Bz/Ag(111), and 0.78 eV for Bz/Cu(111), while the experimental values are 1.10, 0.70, and 1.05 eV for Au, Ag, and Cu, respectively.[12] Our interface dipoles show the same trend than the experimental data, with a minimum dipole potential for the Ag case and a maximum for Au, although our absolute values are a little too small: as commented above this is probably due to the pillow dipole correction that needs to be added to our FIREBALL calculation, and to the different molecule-metal distances, larger for Ag and smaller for Cu. Morikawa and co-workers using a DFT approach[18] have calculated 1.14 eV for Bz/Au(111); 0.76 eV for Bz/Ag(111); and 1.06 eV for Bz/Cu(111), in excellent agreement with the experiments, but the Bz/metal distances [3.1 Å (Au); 3.3 Å (Ag); and 2.9 Å (Cu)] were basically fitted to reproduce the experimental dipoles.

Independently, Bagus and co-workers[12] using a wavefunction-based *ab initio* method and a cluster model have obtained 0.87 eV for Bz/Au(111); 0.77 eV for Bz/Ag(111); and 1.08 eV for Bz/Cu(111), in good agreement with our results. It is worth commenting that, based on a constrained space orbital variation (CSOV) analysis of these calculations, these authors conclude that the observed interface dipole is largely due to the exchange (or Pauli) repulsion between electrons in the metal and in the organic,[12] an observation that seems to be in contradiction with the findings of our work, that indicate that the main mechanism behind the interface dipole formation is the charge transfer between the metal and the organic. A deeper analysis shows, however, that there is no contradiction between these two points of view. First, notice that in a DFT calculation the different wavefunctions are orthogonalized to each other, including in this way the effect of the Pauli repulsion in the interface barrier formation, an effect that automatically leads to a significant charge transfer at the interface; consequently, our DFT FIREBALL calculation includes the "exchange repulsion" effect discussed by Bagus *et al.*, except for the small contribution analyzed above in the "pillow effect" section. Second, notice that in the frozen-orbital step in the COSV analysis, the (Pauli exclusion principle) requirement of orthogonalization of the wavefunctions in the metal and in the molecule already leads to a "major net motion of charge from the adsorbate toward the substrate,"[45] which will appear in our analysis as a charge transfer between the two media.

In conclusion, we have presented a DFT calculation of the interface properties of the benzene/Au(111) interface, introducing a self-consistent analysis of the molecule charging energy and its transport energy gap. From our calculations we have also analyzed other noble metals by changing fictitiously the metal workfunction while keeping the Au electronic properties. Our results have been favourably compared with other theoretical and experimental data, lending strong support to our interpretation of the formation of these interfaces as due to the charge transfer between the metal and benzene, as described in the IDIS-model.

ACKNOWLEDGMENTS

This work is supported by Spanish MICIIN under Contracts No. MAT2007-60966 and No. FIS2010-16046, the CAM under Contract No. S2009/MAT-1467, and the European Project MINOTOR (Grant No. FP7-NMP-228424). E.A. gratefully acknowledges financial support by the Consejería de Educación of the CAM and the FSE. J.I.M. acknowledges funding from Spanish MICINN through Juan de la Cierva Program.

[1] W. R. Salanek, S. Stafstrom, and J. L. Bredas, *Conjugated Polymer Surfaces and Interfaces: Electronic and Chemical Structure of Interfaces for Polymer Light Emitting Diodes* (Cambridge University, Cambridge, 1996).
[2] N. Koch, ChemPhysChem **8**, 1438 (2007).
[3] S. Narioka, H. Ishii, D. Yoshimura, M. Sei, Y. Ouchi, K. Seki, S. Hasegawa, T. Miyazaki, Y. Harima, and K. Yamashita, Appl. Phys. Lett. **67**, 1899 (1995).
[4] I. G. Hill, A. Rajagopal, A. Kahn, and Y. Hu, Appl. Phys. Lett. **73**, 662 (1998).
[5] H. Ishii, K. Sugiyama, E. Ito, and K. Seki, Adv. Mater. **11**, 605 (1999).
[6] I. G. Hill, J. Schwartz, and A. Kahn, Org. Electron. **1**, 5 (2000).
[7] X. Crispin, V. Geskin, A. Crispin, J. Cornil, R. Lazzaroni, W. R. Salaneck, and J.-L. Brédas, J. Am. Chem. Soc. **124**, 8131 (2002).
[8] C. Shen and A. Kahn, Org. Electron. **2**, 89 (2001).
[9] M. Knupfer and G. Paasch, J. Vac. Sci. Technol. A **23**(4), 1072 (2005).
[10] S. Yanagisawa and Y. Morikawa, J. Phys. Condens. Matter **21**, 64247 (2009).
[11] P. Bagus, V. Staemmler, and C. Wöll, Phys. Rev. Lett. **89**, 96104 (2002).
[12] G. Witte, S. Lukas, P. S. Bagus, and C. Woll, Appl. Phys. Lett. **87**, 263502 (2005).
[13] H. Vázquez, Y. J. Dappe, J. Ortega, and F. Flores, J. Chem. Phys. **126**, 144703 (2007).
[14] H. Vázquez, R. Oszwaldowski, P. Pou, J. Ortega, R. Pérez, F. Flores, and A. Kahn, Europhys. Lett. **65**, 802 (2004).
[15] H. Vázquez, F. Flores, R. Oszwaldowski, J. Ortega, R. Pérez, and A. Kahn, Appl. Surf. Sci. **234**, 107 (2004).
[16] M. Betti, A. Kanjilal, C. Mariani, H. Vázquez, Y. J. Dappe, J. Ortega, and F. Flores, Phys. Rev. Lett. **100**, 27601 (2008).
[17] E. Abad, J. Ortega, Y. J. Dappe, and F. Flores, Appl. Phys. A: Mater Sci. Process **95**, 119 (2009).
[18] K. Toyoda, Y. Nakano, I. Hamada, K. Lee, S. Yanagisawa, and Y. Morikawa, Surf. Sci. **603**, 2912 (2009).
[19] S. Kümmeland L. Kronik, Rev. Mod. Phys. **80**, 3 (2008).
[20] F. Flores, J. Ortega, and H. Vázquez, Phys. Chem. Chem. Phys. **11**, 8658 (2009).
[21] E. Abad, C. González, J. Ortega, and F. Flores, Org. Electron. **11**, 332 (2010).

[22]J. D. Sau, J. B. Neaton, H. J. Choi, S. G. Louie, and M. L. Cohen, Phys. Rev. Lett. **101**, 26804 (2008).
[23]E. Abad, J. Ortega, and F. Flores, "Metal/organic barrier formation for a C_{60}/Au interface: from the molecular to the monolayer limit" Phys. Rev. B (submitted).
[24]P. Jelínek, H. Wang, J. Lewis, O. Sankey, and J. Ortega, Phys. Rev. B **71**, 235101 (2005); J. P. Lewis, K. R. Glaesemann, G. A. Voth, J. Fritsch, A. A. Demkov, J. Ortega, and O. F. Sankey, *ibid.* **64** 195103 (2001).
[25]M. Basanta, Y. J. Dappe, P. Jelínek, and J. Ortega, Comput. Mater. Sci. **39**, 759 (2007).
[26]M. Fuchs and M. Scheffler, Comput. Phys. Commun. **119**, 67 (1999).
[27]J. Plíva, J. W. C. Johns, and L. Goodman, J. Mol. Spectrosc. **148**, 427 (1991).
[28]A. Maeland and T. Flanagan, Can. J. Phys. **42**, 2364 (1964).
[29]P. Han, B. A. Mantooth, E. C. H. Sykes, Z. J. Donhauser, and P. S. Weiss, J. Am. Chem. Soc. **126**, 10787 (2004).
[30]Since FIREBALL is a real-space technique there is no practical limitation on the value for the distance between slabs in the z direction; in these calculations we have chosen a distance of 99 Å (so different slabs cannot virtually see each other).
[31]F. Ortmann, F. Bechstedt, and W. Schmidt, Phys. Rev. B **73**, 205101 (2006).
[32]S. Grimme, J. Antony, T. Schwabe, and C. Mück-Lichtenfeld, Org. Biomol. Chem. **5**, 741 (2007); S. Grimme, J. Comput. Chem. **27**, 1787 (2006).
[33]*Handbook of Chemistry and Physics*, edited by D. R. Lide (Chemical Rubber, Cleveland, 1998).
[34]I. Nenner, J. Chem. Phys. **62**, 1747 (1975).
[35]K. Pernal, R. Podeszwa, K. Patkowski, and K. Szalewicz, Phys. Rev. Lett. **103**, 263201 (2009).
[36]J. Ángyán, I. Gerber, A. Savin, and J. Toulouse, Phys. Rev. A **72**, 12510 (2005).
[37]D. C. Langreth, M. Dion, H. Rydberg, E. Schrder, P. Hyldgaard, and B. I. Lundqvist, Int. J. Quantum Chem. **101**, 599 (2005).
[38]N. Marom, A. Tkatchenko, M. Scheffler, and L. Kronik, J. Chem. Theory Comput. **6**, 81 (2010).
[39]M. A. Basanta, Y. J. Dappe, J. Ortega, and F. Flores, Europhys. Lett. **70**, 355 (2005).
[40]Y. J. Dappe, M. Basanta, F. Flores, and J. Ortega, Phys. Rev. B **74**, 205434 (2006).
[41]Y. J. Dappe, J. Ortega, and F. Flores, Phys. Rev. B **79**, 165409 (2009).
[42]G. Savini,Y. J. Dappe, S. Öberg, J. C. Charlier, M. I. Katsnelson, and A. Fasolino, Carbon **49**, 62 (2011).
[43]C. González, J. Ortega, F. Flores, D. Martínez-Martín, and J. Gómez-Herrero, Phys. Rev. Lett. **102**, 106801 (2009).
[44]D. Syomin, J. Kim, B. E. Koel, and G. B. Ellison, J. Phys. Chem. B **105**, 8387 (2001).
[45]P. S. Bagus, K. Hermann, and C. Wöll, J. Chem. Phys. **123**, 184109 (2005).
[46]J. M. Garcia-Lastra, C. Rostgaard, A. Rubio, and K. S. Thygesen, Phys. Rev. B **80**, 245427 (2009).